

# Hydraulic Jump Formation in Water Sloshing Within an Oscillating Tank

Peter J. Disimile\*

*University of Cincinnati, Cincinnati, Ohio 45221*

and

John M. Pyles<sup>†</sup> and Norman Toy<sup>‡</sup>

*Engineering and Scientific Innovations, Inc., Blue Ash, Ohio 45241*

DOI: 10.2514/1.38493

An experimental investigation on the formation of dynamic hydraulic jumps in an oscillating rectangular container was performed using a high-resolution, high-speed digital imaging system. The present work investigates driven angular roll oscillations using a state-of-the-art motion simulator and a transparent rectangular container. A hydraulic jump was observed traversing between the walls of the tank when the container was oscillated near the surface-wave resonance frequency based on liquid depth. The hydraulic jump was imaged and its characteristics were measured using image processing software. It was found that the directionally based hydraulic jump formation frequency matches the driven frequency. However, the phase difference between the two is dependent on the ratio of the driven frequency to resonance frequency. Furthermore, the spatial characteristics of the jump are dependent on the amplitude and frequency of the oscillation.

## Nomenclature

$A$	=	simulator offset
$B$	=	tank length, m
$f$	=	driven frequency, Hz
$f_0$	=	resonant frequency, Hz
$g$	=	gravitational acceleration constant, 9.8 m/s <sup>2</sup>
$H$	=	tank height, m
$h_0$	=	initial depth, m
$R$	=	correlation coefficient
$t$	=	time, s
$y_{\max}$	=	maximum tank deflection distance, m
$\eta$	=	wave height with respect to initial depth, m
$\theta$	=	tank angle, deg
$\theta_0$	=	oscillation amplitude, deg
$\lambda$	=	tank phase, deg
$\omega$	=	angular frequency, rad/s

## Introduction

**L** IQUID dynamics in moving containers is of special interest to air, marine, and ground vehicles, due to the movement of the liquid, or slosh, in the container and the resulting impact forces it produces on the walls of the container. Slosh can influence the stability and control systems of air vehicles, and care must be taken when designing a tank so that the sloshing impact forces can be controlled [1–3]. Furthermore, sloshing in partially filled liquid containers can significantly alter the motion of cargo ships [4,5] and has also been shown to enhance the flammability limits of jet fuel, especially at the lower flammability limit [6,7]. Studies on liquid sloshing note the formation of a nonlinear multiphase event characterized by an air/liquid turbulent region when the vessel is

oscillated at the resonance frequency of the liquid in the container. This phenomenon is known as a hydraulic jump.

A hydraulic jump is characterized by a rapid change in liquid depth with a turbulent region between the two depths and can be classified as either stationary or dynamic [8]. Stationary hydraulic jumps typically form in channel flows with a static location at which the flow transitions from a supercritical to subcritical state. Dynamic hydraulic jumps similarly represent this flow transition; however, their location and physical characteristics constantly change. Both types of hydraulic jumps consist of distinct flow regimes and spray regions (Fig. 1).

At the base of a hydraulic jump, an entrained air shear layer forms and propagates the length of the jump. Above this shear layer are multiple recirculation regions in which a great deal of liquid/air mixing occurs. At the top of the jump, three distinct spray regions are produced: an aerosol/fog region, a spray/mist region, and a large-droplet region [9]. However, the latter research used intrusive measurements that are not appropriate for dynamic environments in which the physical properties of the jump could be altered by the measurement device.

A review of the literature shows a distinct void in experimental investigations into dynamic hydraulic jumps, although there are a number of theoretical investigations using various methods for attempting the modeling and prediction of such dynamic hydraulic jumps. In a model by Verhagen and van Wijngaarden [10], the Chu–Ying–Lin method was applied and is based on a theoretical analysis of resonance oscillations in a gas column that allowed the formation of a shock wave to be modeled as a mathematical discontinuity [11,12]. The technique was adapted for an analysis on hydraulic jump formations at or near the resonance frequency of the liquid, with the hydraulic jump being the equivalent of a shock wave in gas dynamics. This model was compared with a small-scale experiment conducted by the researchers, and some agreement was noted for shallow liquid depths and oscillation amplitudes below 4 deg. This study remains one of the few published experimental investigations on dynamic hydraulic jumps.

Since this research, many models have been constructed with little experimental validation employing different mathematical treatments, such as potential flow theory [5], Glimm’s method [13,14], finite element method [15], and finite difference method [16]. Many of these models had limitations related to modeling of liquid dynamics with tank-oscillation amplitudes greater than 1 deg [16] or with the liquid depth approaching the length of the tank [5]. Such numerical schemes have difficulty with the depth discontinuity

Received 11 May 2008; accepted for publication 8 November 2008. Copyright © 2008 by the American Institute of Aeronautics and Astronautics, Inc. All rights reserved. Copies of this paper may be made for personal or internal use, on condition that the copier pay the \$10.00 per-copy fee to the Copyright Clearance Center, Inc., 222 Rosewood Drive, Danvers, MA 01923; include the code 0021-8669/09 \$10.00 in correspondence with the CCC.

\*Associate Professor, Department of Aerospace Engineering, P.O. Box 210070.

<sup>†</sup>Research Engineer, 4625A Carlyn Drive.

<sup>‡</sup>Chief Engineer, 4625A Carlyn Drive.

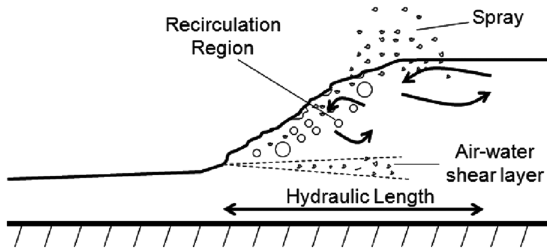


Fig. 1 Regions of a hydraulic jump.

introduced by the hydraulic jump and, with the limited experimental data available for validation purposes, are prone to misinterpretation. Furthermore, they also have difficulty predicting the phase of the hydraulic jump and therefore cannot predict the location of the hydraulic formation [13].

Although there are numerous theoretical models that attempt to provide an accurate portrayal of the complex liquid dynamics within a partially filled oscillating container, the lack of experimental research on this phenomena does not provide for such models to be validated. The current research determines the minimum limiting tank-oscillation parameters that yield hydraulic jumps and applies image analysis of flow visualization to quantify several spatial characteristics of the hydraulic jump. The scale of this research allows for the results to be applied to numerous practical applications on the same order when the mass of liquid, container size, and environment are markedly similar. The goal of this research is to use visual data coupled with spatial measurements to assist with furthering the theoretical models of a liquid in a partially filled container through the use of nondimensional characteristic parameters describing the driven-tank oscillation as well as the resulting hydraulic jump. Furthermore, this research aims to enhance the understanding of past research when the formations of hydraulic jumps are undesirable.

### Theoretical Considerations

As mentioned in the previous section, numerous theoretical studies provide insight into the necessary oscillation conditions that produce hydraulic jumps. For this present study, the coordinate system shown in Fig. 2 was considered [10]. Two coordinate systems provide a theoretical basis for characterizing the liquid free surface in the tank, coupled with the motion of the test fixture. These coordinate systems will also be referred to when discussing shallow-water flow theory.

The coordinate systems contain the stationary coordinate system of  $O-x_0y_0$  and the moving coordinate system of  $G-xy$ , which rotates about the origin  $O$ . The moving coordinate system moves with the tank, with its origin  $G$  located at the center point on the base of the tank. The inclination angle of the tank is given as  $\theta$ , and the surface height relative to the initial rest surface in the dynamic coordinate system is represented as  $\eta$ . The rest height of the fluid from the fixed coordinate system is denoted as  $H$ , and the rest height of the liquid

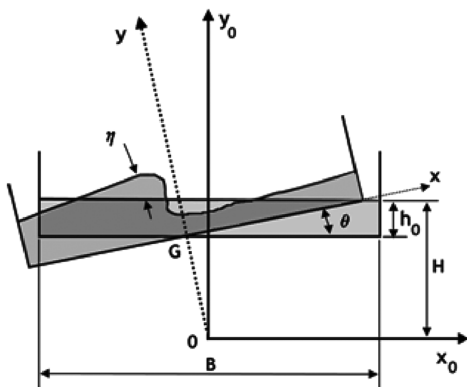


Fig. 2 Coordinate system for the oscillating tank.

from the bottom of the tank is denoted by  $h_0$ . Three-dimensional effects will not be analyzed in this study.

For shallow depths at which  $h_0 \ll B$ , shallow-water wave theory [17] can be used to model the liquid-surface height [10]. It was found that the liquid-surface height function is not defined when the driven frequency of the tank approaches the resonance frequency  $f_0$  of the liquid depth [10,13], as defined in Eq. (1):

$$f_0 = \frac{(gh_0)^{1/2}}{2B} \quad (1)$$

### Methods and Materials

A complete description of the testing facility and setup is described in [18], and a brief synopsis is presented in the current section. To replicate generic roll aircraft dynamics, a hydraulically activated Sarnicola Hexad AIES six-degree-of-freedom motion simulator was employed. The platform of this motion simulator, shown in Fig. 3, has six degrees of freedom provided by six hydraulic actuators controlled through proprietary computer software, was designed to replicate aircraft maneuvers, and, for the purpose of this research, served in replicating a rolling oscillation of an aircraft wing.

Typically, fuel is stored between several baffled regions within an aircraft wing, as shown diagrammatically in Fig. 4. To replicate a single baffled section of the wing fuel tank, a rectangular container was constructed that provided optical access to three spatial planes through the top, side, and front. The optical access surfaces were constructed of Lexan, with the other walls fabricated from steel.

The tank had overall internal dimensions of 1.9 m (73 in.) by 1.2 m (48 in.) by 0.94 m (37 in.), yielding a maximum capacity of 2.1 m<sup>3</sup> (563 gal), and will provide a larger test article than in past experiments, as discussed in the previous section [10]. To provide extra support to the walls of the tank while undergoing dynamic fluid motion, a steel skeletal structure surrounded the container and was constructed of 6.35-mm-thick (0.25-in.-thick) steel tubing. A SolidWorks Model of the entire tank and simulator setup is shown in Fig. 5 with corresponding dimensions.

The dynamic motion of the fluid in the container undergoing a rolling motion was visualized and analyzed using a high-speed

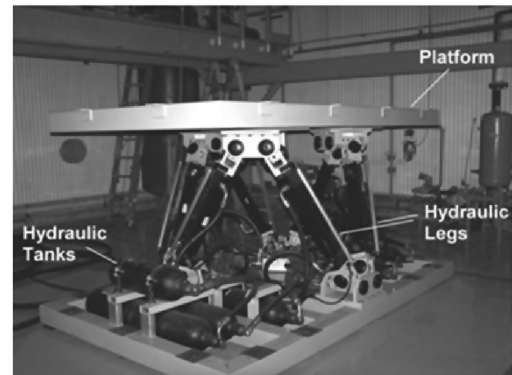


Fig. 3 Six-degree-of-freedom motion simulator.

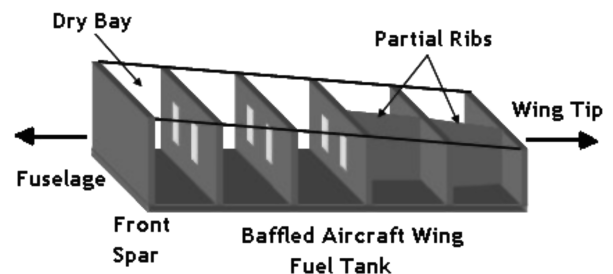


Fig. 4 Typical construction of baffled fuel tanks within an aircraft wing.

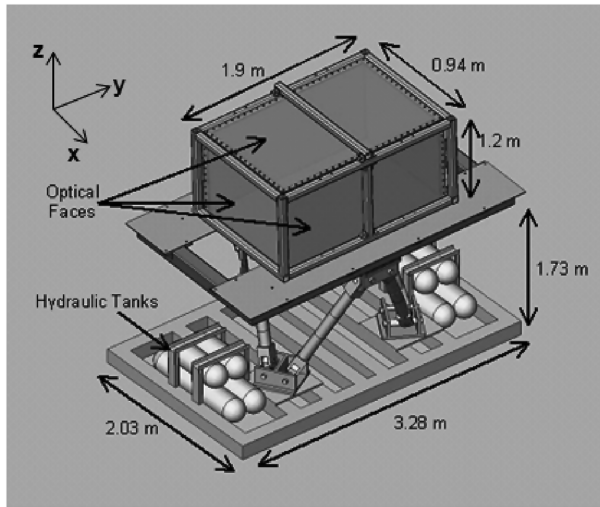


Fig. 5 Diagrammatic sketch of simulator and slosh tank.

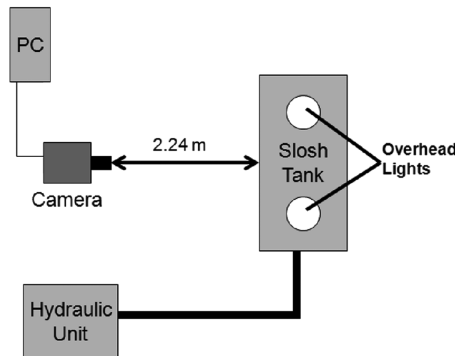


Fig. 6 Arrangement of test facilities.

digital complementary-metal-oxide-semiconductor camera, high-power lights, and in-house software developed for a PC. The camera had a resolution of  $1280 \times 1024$  pixels and was positioned at a height of 1.93 m (76 in.) at a distance of 2.24 m (88 in.) from the front wall of the tank fixture. Two 500 W overhead lights were positioned above the tank to illuminate the flow, and a 20 mm lens was attached to the camera and captured the full field of view of the test apparatus. The digital imaging system acquired video at 75 Hz for a total of 15 s at the start of the oscillation. Because preventing the initial formation of a hydraulic jump in liquid-cargo containers is critical in transport-container design, the current research focused on the transient startup condition. All images were stored in the onboard camera memory and then transferred to the computer via the USB 2.0 connection upon completion of each test for analysis. The complete test setup is shown diagrammatically in Fig. 6.

### Test Conditions

Three liquid depths of water were selected for the examination of liquid-separation phenomena in oscillating containers and are shown in Table 1, along with the resonance frequency based on depth calculated from Eq. (1). These depths were selected based on their

Table 1 Liquid depths and fundamental resonance frequency [Eq. (1)]

Liquid depth, m	Resonance frequency, Hz
0.265	0.42
0.371	0.50
0.530	0.60

low resonance frequencies and are on the fringe of shallow-water wave-theory approximation and have practical implications.

The tank was oscillated at frequencies ranging between 0.20–0.35 Hz for the 0.265 m depth, 0.25–0.40 Hz for the 0.371 m depth, and 0.25–0.50 Hz for the 0.530 m depth at specific maximum tank deflection angles  $\theta_0$  of 2.42, 3.50, and 4.71 deg. Furthermore, the tank oscillation was started at the maximum deflection angle, with care taken to ensure that the fluid was static before starting the oscillation. This prevents any transient effects from the shifting of the tank to the initial angle that could affect the formation characteristics of the hydraulic jump. The oscillation frequency was incremented at steps of 0.05 Hz. The roll angle of the tank,  $\theta$ , as a function of time is described in Eq. (2) for each liquid depth, at which a slight offset  $A$  had to be introduced due to a bias in the motion simulator when the center of gravity was shifted from its manufactured position. The asymmetry of the materials (steel and Lexan) of the tank walls caused this shift in the center of gravity:

$$\theta(t) = \theta_0 \sin(\omega t - \lambda) + A \quad (2)$$

### Results

The flow visualization and data analysis strategy used to examine and characterize hydraulic jumps in the oscillating tank employed a calibration coefficient of 1.8 mm/pixel to the digitized images, with the angle of the tank at the time of the jump formation being determined from observations of the angular position  $\theta$  of the corners of the tank. However, it should be noted that the dynamics of the flow have been considered two-dimensional for the purposes of the following analysis. Although it is recognized that the flow within the jump and along the side walls would be three-dimensional, the location of the jumps were, to first-order approximation, considered as a two-dimensional wave propagating across the tank. Overhead visual observation of the dynamic fluid motion in the tank affirmed this assumption. The length of the tank was also measured in each hydraulic jump image to ensure the accuracy of the results. Because the length of the tank is known to be 1.90 m, this was used as a baseline for the accuracy of the measurement technique. As a result, it was found that the spatial measurements are within a 2% uncertainty.

### Hydraulic Jump Formation

It was found that when the tank was oscillated at a driven frequency near the resonance frequency, a hydraulic jump was observed traversing between the walls of the tank. The formation of the jump is shown in the following digital images from a 0.265 m liquid-depth test, oscillated at a roll amplitude of 4.71 deg and a frequency of 0.30 Hz. A surface wave forms at the start of the oscillation of the tank, shown in Fig. 7. This wave propagates against the incoming flow direction. The speed of this wave increases and the top of the wave begins to move at a greater speed than that at the bottom of the wave. This occurs due to the residual fluid moving in the opposite direction of the propagating surface wave (Fig. 8). As a result, the wave breaks and air is entrained into the liquid (Fig. 9), producing a hydraulic jump that is characterized by a rapid change in depth, separated by a turbulent region and the ejection of spray from the surface (Fig. 10).

Note that three types of hydraulic jump conditions were observed. The first type was a single jump that typically formed at the lower-frequency oscillation during the second rotation of the tank. The formation of subsequent jumps was inhibited by the spray from the impact of the initial hydraulic jump on the end wall. The second type of jump condition was a transitional jump that only occurred on the clockwise rotation of the tank (one jump per oscillation period). Similar to the single-jump condition, the spray from the incident jump inhibited the formation of the subsequent jump. However, the reflection of the subsequent wave off of the opposite end wall with limited spray allowed the wave to continue to accelerate and form a hydraulic jump. The final condition observed was an oscillatory condition in which hydraulic jumps formed on each rotation and

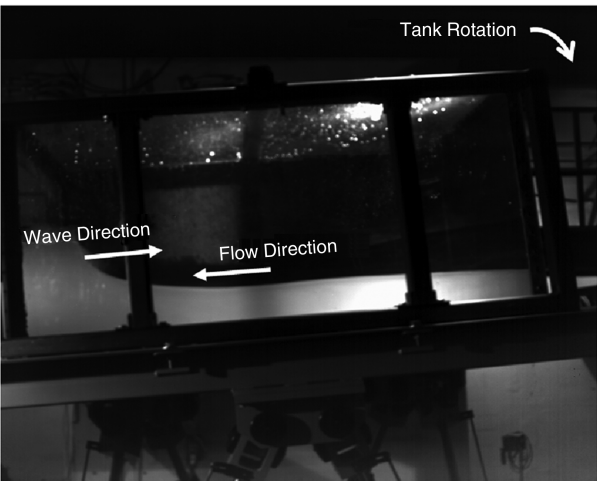


Fig. 7 Initial formation of wave.

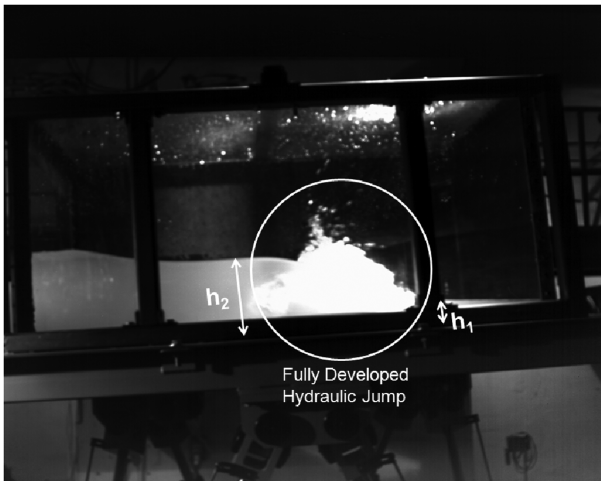


Fig. 10 Fully developed hydraulic jump and spray ejection.

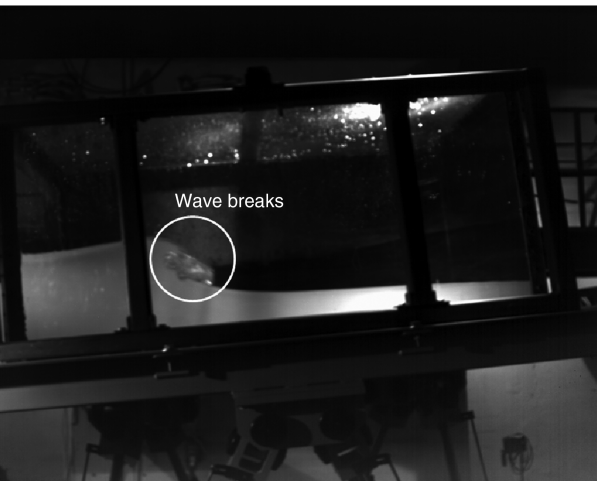


Fig. 8 Breaking of wave/start of hydraulic jump formation.

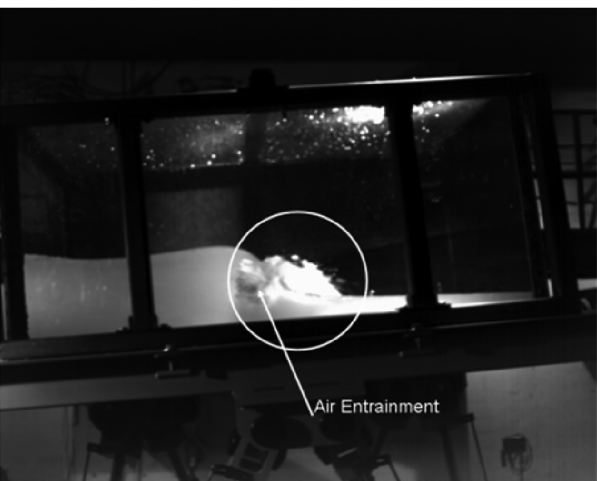


Fig. 9 Continued development of hydraulic jump showing air entrainment.

counter-rotation of the tank. This typically occurred on the near-resonant oscillation frequencies and/or large oscillation amplitudes. In each of the two lower depths, hydraulic jumps were only observed at the frequencies shown in Table 2 for different roll angle amplitudes, whereas the upper depth did not exhibit a hydraulic jump. The 0.265 m depth exhibited hydraulic jump formations for

oscillation frequencies of 0.30 and 0.35 Hz at all three of the tested amplitudes. The 3.50- and 4.71-deg-amplitude cases produced a single hydraulic jump after the first tank oscillation at the 0.25 Hz oscillation frequency, whereas the 2.42 deg exhibited a single-jump condition at the 0.30 Hz oscillation frequency. A transitional condition was observed at an oscillation amplitude of 3.50 deg and frequency of 0.30 Hz for this depth. Oscillation frequencies above 0.35 Hz were not tested as part of the current research. When the depth was increased to 0.371 m, fewer tested frequencies produced hydraulic jumps.

Hydraulic jumps were not observed in the 2.42-deg-amplitude tests for frequencies up to 0.40 Hz for this depth. The 3.50-deg-amplitude condition produced only left-to-right traveling jumps at a frequency of 0.40 Hz, with its reflected counterpart not being observed. The 4.71 deg amplitude produced oscillatory jumps (incident and reflected jumps on the rotation and counter-rotation of the tank) for the 0.35 Hz condition and single jumps for the 0.30 Hz oscillation frequency. Frequencies above 0.35 Hz were not tested for this roll amplitude because two lower-frequency conditions yielded hydraulic jumps, and the goal of the current research was to determine the minimum driven oscillation factors conducive to hydraulic jump formation.

Finally, at a depth of 0.530 m (approximately half the height of the tank), hydraulic jumps were not observed for test frequencies up to 0.50 Hz. Although this frequency is near the resonant frequency of the depth (0.60 Hz), limitations in the height of the tank prevented the formation of a hydraulic jump. The top of the tank prevented the initial wave from reflecting off of the end wall. As the wave interacted with the end wall, it would impact the upper wall and disrupt the reflection of the wave. This suggested that for an enclosed tank, the tank height must be greater than two liquid depths for hydraulic jump formation to occur.

Location of the Hydraulic Jump

The location at which a fully developed hydraulic jump occurs as the tank undergoes oscillation was determined from measuring its

Table 2 Driven frequencies at which hydraulic jump formation was observed

Roll angle amplitude	2.42 deg	3.50 deg	4.71 deg
0.265 m	0.30, 0.35 Hz	0.25, 0.30, 0.35 Hz	0.25, 0.30, 0.35 Hz
0.371 m	None (<0.40 Hz)	0.40 Hz	0.30, 0.35 Hz
0.530 m	None (<0.50 Hz)	None (<0.50 Hz)	None (<0.50 Hz)

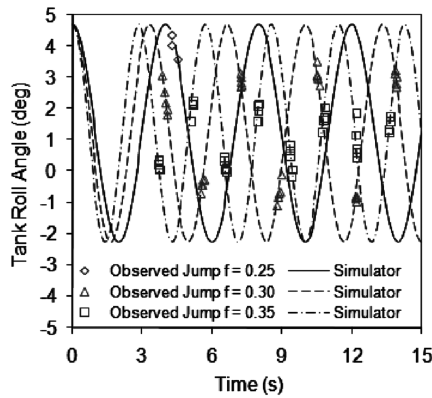


Fig. 11 Hydraulic jump formation for 0.265 m depth and 3.50 deg roll amplitude.

position with respect to the angle of the tank at a specific time in its trajectory. Figure 11 shows a typical graphical result of the location of hydraulic jumps in 0.265 m depth as the tank is oscillated at an amplitude of 3.50 deg for oscillation frequencies of 0.25 Hz (solid line), 0.30 Hz (dashed line), and 0.35 Hz (dotted-dashed line). Hydraulic jumps were not observed during the first oscillation. This was due to the fluid initially starting at rest at the inclined angle and requiring at least one oscillation to establish the liquid flow conditions and provide sufficient kinetic energy to the liquid through the driven-tank motion.

Although fully developed hydraulic jumps were first observed at a driven frequency of 0.25 Hz, only three jumps were recorded out of ten analyzed tests at this frequency. In this case, the formation of each of the jumps occurred after the first oscillation of the tank (shown by the diamond data points in Fig. 11) and did not occur during the remainder of the tank motion.

For the 0.30 Hz (triangular data points) and 0.35 Hz (square data points) oscillation configurations, hydraulic jumps occurred on the clockwise and counterclockwise rotation of each cycle of the tank, but only after the initial cycle. For these frequencies, this occurred for five consecutive tests at each frequency and no further tests were analyzed. It was observed that the hydraulic jump formation appears to oscillate at the same frequency with the tank, but notably out of phase with the driven-tank oscillation. Furthermore, the angle of the tank at which the hydraulic jump form changes with the tank frequency. Most notable is the difference in the hydraulic jump formation oscillation between the 0.30 and 0.35 Hz conditions. Between the two frequencies, the hydraulic jump oscillation appears to invert, with the first hydraulic jump in the 0.30 Hz condition forming near the maximum tank angle and the initial hydraulic jump in the 0.35 Hz condition forming near the minimum tank angle.

### Height of the Hydraulic Jump

The hydraulic height of each of the jumps was measured using digital imaging software. A typical hydraulic jump height profile is shown in Fig. 12. This profile, from the 0.265 m depth and 0.35 Hz configuration, shows the height of the hydraulic jump when it first forms in the tank on each oscillation.

The height of each hydraulic jump appears to oscillate throughout the tank motion, and it is suggested that the spray from the wall impact of the previous hydraulic jump affects the formation of the subsequent jump. Also of note is that the increased amplitude of the oscillation increases the hydraulic height of the jump, due to the increased gravitational force.

The height of the hydraulic jump was normalized by the initial depth of the liquid. The effect of the initial liquid depth on the normalized hydraulic height was examined by comparing the average hydraulic jump height for the 0.265 and 0.371 m depths (recall that the 0.530 m depth did not exhibit a hydraulic jump). Figure 13 shows the hydraulic height of each jump throughout the oscillation at a 4.71 deg amplitude and 0.35 Hz and shows that the hydraulic jumps appears to form slightly earlier in the tank oscillation

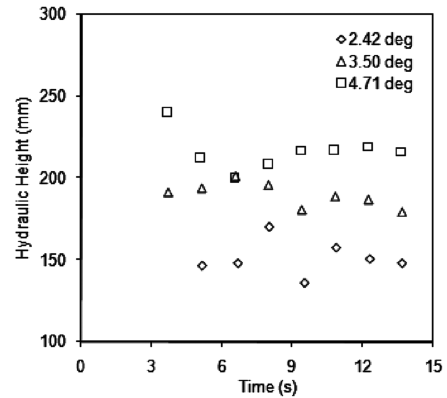


Fig. 12 Hydraulic heights for the 0.265 m depth at 0.35 Hz frequency.

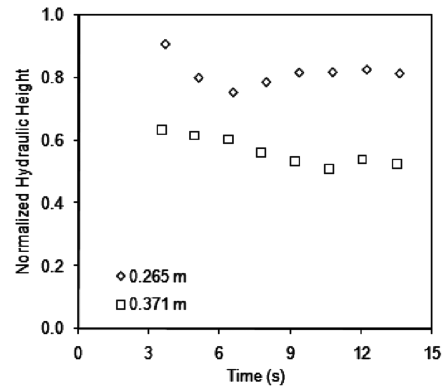


Fig. 13 Hydraulic height for two depths at 4.71 deg amplitude and 0.35 Hz frequency.

for the deeper fluid. Furthermore, it also demonstrates the complexities of the hydraulic jump formation. Different temporal variations in the normalized height are observed between the two volumes despite having similar tank-oscillation conditions. This suggests that the spray volumes produced from the initial hydraulic jump have a significant effect on the formation of the subsequent jump. The effect is greater when the hydraulic jump height is a greater percentage of the initial liquid depth, due to greater spray production. This notion is not often reflected in sloshing models.

Furthermore, similar trends in the hydraulic jump height variation with time were observed for the two depths, with an oscillatory pattern appearing for both depths. From Fig. 13, the difference in the normalized hydraulic jump heights between the depths varied by as little as 20% for the jump at 6.4 s into the oscillation and by as much as 38% for the jump formed 10.7 s into the oscillation.

The average hydraulic height measured for each of the oscillation conditions was determined. Each oscillation condition was then normalized by the ratio of the maximum vertical deflection distance of the tank oscillation ( $y_{\max}$ ) to the initial depth of the liquid ( $h_0$ ) multiplied by the ratio of the driven frequency  $f$  to the theoretical resonance frequency  $f_0$  [Eq. (1)]. An expression of the normalized oscillation condition is shown next:

$$\frac{y_{\max}}{h_0} \times \frac{f}{f_0} \quad (3)$$

When the normalized hydraulic height is plotted against the normalized oscillation condition for the tested depths, an approximately linear trend is observed (Fig. 14). This trend suggests a correlation between the factors in Eq. (3) and the size of the hydraulic jump. Furthermore, it suggests that larger jumps are observed near the resonance frequency of the liquid depth at large deflection angles. This is consistent with theory, as the strength of the jump (or height) should increase with increasing gravitational force

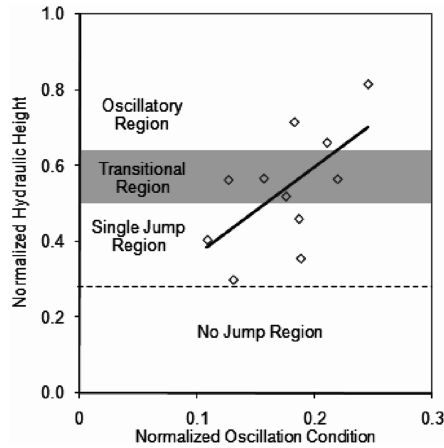


Fig. 14 Normalized hydraulic height for given normalized oscillation condition.

(or tank roll amplitude). Also, the strongest jumps should be observed at the resonance frequency of the liquid. Until now, the effects these parameters have on the hydraulic jump characteristics have not been measured. In addition to this relation, a secondary trend was also observed relating the size of the hydraulic jump and the nature of the jump oscillation.

As suggested by Fig. 13, the formation of the initial jump and its impact on the end walls has an effect on the formation of the subsequent jump. In this test series, the observed hydraulic height effect yielded three distinct regions. Normalized heights approximately between 0.3 and 0.5 typically only produced a solitary jump near the beginning of the oscillation. The impact of this jump on the end wall and resultant spray disturbed the propagation of the reflected surface wave, reducing the energy of the reflected wave below critical flow conditions.

Within the transitional region (normalized heights between 0.5 and 0.65), multiple jumps were observed during the oscillation; however, they typically were monodirectional. Similar to the single-jump case, the spray from the previous jump reduced the energy of the reflected surface wave below critical conditions, inhibiting the formation of an opposite-traveling subsequent jump. When this wave reflected off of the opposite end wall, normally yielding little spray, the inertial force of the wave is increased due to the counter-rotation of the tank. This results in a critical-to-supercritical wave, resulting in a hydraulic jump. This process is repeated throughout the oscillation. Above this region is an oscillatory region in which hydraulic jumps are typically large and occur during each rotation and counter-rotation of the tank near-resonant frequency conditions.

The hydraulic height-to-length ratio (Fig. 1) was measured from the digital video as a function of the time after the initial jump forms (presented in Fig. 15) and provides insight into how the physical characteristics of the hydraulic jump evolve from the time it forms to the time it impacts the end wall.

The larger of the two lower depths, 0.371 m, produced a steeper initial jump than the smaller depth. However, the height-to-length ratio of the jump in the larger depth quickly decreased as it neared the end wall of the tank. The height-to-length ratio of the jump in the 0.265 m depth decreased at a slower rate. This may be caused by the jump in the larger depth being a weaker jump and therefore not being as stable. The 0.265 m depth has an additional data point in Fig. 15, because the jump formed earlier in the oscillation and therefore had not reached the end wall 0.20 s after it formed. Both sets of data suggest a linear trend in the hydraulic height-to-length ratio with time. The high correlation coefficients for each liquid depth suggest a constant change in the physical properties of the jump from the time it forms to the time it interacts with the end walls of the tank.

#### Froude Number

Typically, hydraulic jumps such as those formed in shallow channels are characterized by a nondimensional parameter known as

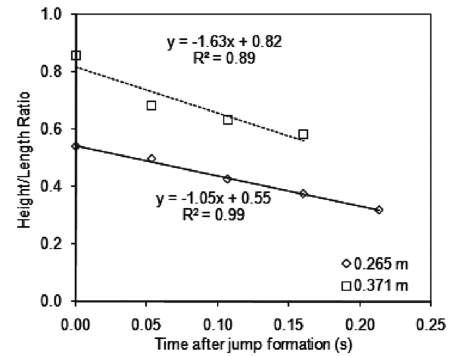


Fig. 15 Hydraulic height/length ratio for two depths at a 0.35 Hz oscillation frequency.

the Froude number  $Fr$ . This characteristic number relates the ratio of the inertial forces to the gravitational forces for a given flow condition. A hydraulic jump forms when the inertial forces of a wave exceed the sustainable wave speed, or wave celerity, for a given liquid depth, yielding a Froude number greater than unity. This is known as supercritical flow, whereas flows with Froude numbers less than 1 are called subcritical. Characteristic of subcritical and supercritical flows is the direction of propagating surface waves. In subcritical flows, the surface-wave propagation occurs with and against the fluid flow. On the other hand, waves in supercritical flows propagate with the flow direction at a velocity greater than the wave celerity of the flow depth [19]. Typically, the Froude number can give an indication into the relative strength of the hydraulic jump, with larger Froude numbers indicating a jump with greater energy dissipation.

The Froude number for each visualized hydraulic jump was determined using a numerical expression derived by Defina and Susin [20] based on the measured upstream and downstream hydraulic jump depth for upward-sloping channels. Table 3 shows the average Froude numbers of the hydraulic jumps for each oscillation condition. The  $\times$  in the table denotes that a test was conducted at this condition but a hydraulic jump was not observed, although bidirectional surface waves were present, indicating a subcritical flow condition ( $Fr < 1$ ). A test was not conducted for the case of the 0.371 m depth, 4.71 deg amplitude, and 0.40-Hz-frequency oscillatory condition, because jumps were observed at two lower-frequency conditions. The table illustrates that the Froude number is dependent on not only the frequency of the oscillation, but the amplitude as well. For example, the 3.50 deg amplitude and 0.35 Hz oscillation frequency (0.265 m depth) yielded multiple jumps with an average Froude number of 2.5, whereas an oscillation condition of 4.71 deg amplitude and 0.30 Hz oscillation frequency yielded stronger jumps ( $Fr = 2.8$ ) despite this oscillation frequency being further from a resonant condition. The table also suggests that to have a hydraulic jump formation, the oscillation frequency must approach the resonant frequency as the oscillation amplitude is reduced.

As suggested in Table 3, the characteristic Froude number and relative strength of the hydraulic jump are dependent on multiple parameters involving the nature of the tank oscillation. When the Froude number is plotted against the normalized oscillation condition [Eq. (3)] (Fig. 16a) and the normalized hydraulic height

Table 3 Hydraulic jump Froude numbers

Test condition		Amplitude		
Depth	Frequency, Hz	2.42 deg	3.50 deg	4.71 deg
0.265 m	0.25	$\times$	1.4	2.1
	0.30	1.6	2.1	2.8
	0.35	1.8	2.5	3.1
0.371 m	0.30	$\times$	$\times$	1.5
	0.35	$\times$	$\times$	2.1
	0.40	$\times$	1.7	No test

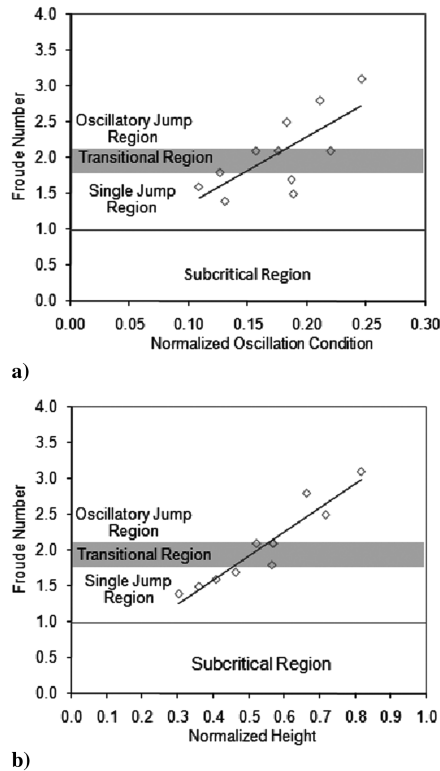


**Fig. 16 Froude number variation for a) different oscillations and b) hydraulic jump conditions.**

(Fig. 16b), clear trends can be observed. In Fig. 16a, the expected result of stronger hydraulic jumps forming near-resonant oscillation conditions is observed. In addition, the figure also demonstrates that the strength of the hydraulic jump affects the nature of the liquid oscillation. Lower Froude numbers often result in oscillation conditions that only produce a single hydraulic jump during the second oscillation of the tank. Higher Froude numbers tend to result in hydraulic jump formation during the rotation and counter-rotation of the tank for each oscillation. This tends to occur for oscillations near resonance frequency and/or high-oscillation amplitudes. This notion is also reflected in Fig. 16b, with a much higher correlation being observed.

## Conclusions

High-speed, high-resolution imaging systems were used for flow visualization and spatial measurements of dynamic hydraulic jumps in oscillating tanks using water as the specimen fluid. When the tank was oscillated at a frequency near the theoretical resonance frequency of the liquid depth, a hydraulic jump was observed. This jump formed at the same frequency as the driven-tank frequency but was out of phase with the driven oscillation. Each oscillation condition produces hydraulic jumps with unique spatial characteristics that have not been previously measured.

Quantification of the flow images was also able to provide accurate spatial measurements of each hydraulic jump not seen in numerical studies. These results show that increasing the amplitude of the oscillation also increases the height of the hydraulic jump. If the amplitude is doubled, an increase between 25 and 40% in the hydraulic height was observed, due to the increased inclination angle of the tank, resulting in greater shifting of the liquid. As a result, a drastic depth change occurs across the surface wave. This causes the increased size in the hydraulic jump due to the need for the jump to dissipate a greater amount of energy. Furthermore, the height of each jump appears to oscillate throughout the tank oscillation, suggesting that spray from the previous jump impact on the end wall of the tank affects the height of the following jump.

For the depths and oscillation conditions studied in this research, the ratio of the hydraulic height to the rest depth of the liquid was measured. A stark contrast in the normalized hydraulic height was observed between the two depths. The shallower depth produced normalized heights between 0.75 and 0.91, whereas the 0.371 m depth had normalized heights ranging between 0.52 and 0.63. Although the two depths were tested at the same oscillation conditions (amplitude and frequency), the shallower depth produced higher normalized heights, due to the driven oscillation frequency being near the resonance frequency of the shallow depth. The spatial heights, however, were similar, suggesting an independence of depth on the hydraulic height of a jump at a given frequency. When the oscillation condition was normalized (Fig. 14), a linear trend in the hydraulic height was observed as the oscillation condition approached the resonance frequency at a high deflection angle. This new insight into the spatial characteristics of a hydraulic jump can aid in enhancing the numerical models that only predict the location of hydraulic jumps and not their size.

The evolution of the spatial characteristics of the jump was also measured (Fig. 15). As the jump progresses toward the tank end walls, it grows longer in length, whereas the height of the jump decreases. Several of these spatial characteristics can provide insight into the strength of the hydraulic jumps, which is crucial for container design for land-, air-, and sea-based vehicles.

The strength of a hydraulic jump is often reflected in the nondimensional characteristic Froude number. Conditions that produce higher Froude number hydraulic jumps tend to be less affected by the liquid dynamics induced by the previous impacting hydraulic jump. The data suggest that this type of oscillatory condition can occur for oscillation frequencies near resonance and/or large oscillation amplitudes, as shown in Fig. 16. Furthermore, large-angle oscillations can produce hydraulic jumps with higher Froude numbers at lower oscillation frequencies, showing a significant dependence on oscillation amplitude, even at small angles. Small-angle approximations are typically used in oscillating tank models, whereas the experimental data suggest that even a 1 to 2 deg increase in oscillation amplitude can have significant effects on the jump formation, performance, and type of liquid-motion condition.

Note that these jumps form in the early critical phase at the start of the oscillation when hydraulic jumps are not desirable. They may not represent the steady-state jump characteristics after several oscillations. However, the liquid dynamics during the transient initial oscillation phase are parameters that are crucial for liquid-cargo tank design and for understanding how to prevent the formation of the transient jump during the start of an undesirable oscillation. Steady-state results may reduce the scatter in the current data, yet the transient results still portray the predominant features of the dynamic hydraulic jump accurately. The difference between the transient startup phase and steady-state phase will be examined under future programs.

The viscosity of the specimen fluid was not considered under the current program, but this parameter may have an effect on the hydraulic jump performance. Fluids with high viscosity may not be as conducive to forming hydraulic jumps as water, due to their resistance to flow and produce surface waves. Care must be noted when applying the current results to sloshing models involving other specimen fluids. Fluids such as hydrocarbon fuels and oil are of interest for this type of study, due to their prevalence in different shipping methods, and will be considered in future projects.

Because numerous studies have focused on theoretically predicting and characterizing hydraulic jumps in oscillating containers, the current research provides valuable experimental data for the validation of such computational models.

## Acknowledgments

The authors would like to thank the funding support from the U.S. Department of Defense, the Joint Aircraft Survivability (JAS) program office, and Marty Lentz of the U.S. Air Force 780 Test Squadron, Aerospace Survivability and Safety Flight at Wright-Patterson Air Force Base.

## References

- [1] Abramson, H. N. (ed.), "The Dynamic Behavior of Liquids in Moving Containers," NASA SP-106, 1966.
- [2] Fontenot, L. L., "Dynamic Stability of Space Vehicles: Volume 7—The Dynamics of Liquids in Fixed and Moving Containers," NASA CR-941, Mar. 1968.
- [3] Graham, E. W., and Rodriguez, A. M., "The Characteristics of Fuel Motion Which Affect Airplane Dynamics," Douglas Aircraft Co., Inc., SM-14212, Santa Monica, CA, Nov. 1951.
- [4] Armenio, V., and La Rocca, M., "On the Analysis of Sloshing of Water in Rectangular Containers: Numerical Study and Experimental Validation," *Ocean Engineering*, Vol. 23, No. 8, 1996, pp. 705–739. doi:10.1016/0029-8018(96)84409-X
- [5] Journee, J. M. J., "Fluid Tanks and Ship Motions," Delft Univ. of Technology, Rept. 1237, Delft, The Netherlands, 2000.
- [6] Nestor, L. J., "Investigation of Turbine Fuel Flammability Within Aircraft Fuel Tanks," Naval Air Propulsion Test Center, Aeronautical Engine Department, Rept. DS-67-7, Philadelphia, 1967.
- [7] Ott, E. E., "Effects of Fuel Slosh and Vibration on the Flammability Hazards of Hydrocarbon Turbine Fuels Within Aircraft Fuel Tanks," U.S. Air Force Aero Propulsion Lab., Rept. AFAPL-TR-70-65, Wright-Patterson AFB, OH, 1970.
- [8] Chaudhry, M. H., *Open Channel Flow*, Prentice Hall, Englewood Cliffs, N. J., 1993, pp. 1–63.
- [9] Chanson, H., "Bubble Entrainment, Spray and Splashing at Hydraulic Jumps," *Journal of Zhejiang University Science A*, Vol. 7, No. 8, Jan. 2006, pp. 1396–1405. doi:10.1631/jzus.2006.A1396
- [10] Verhagen, J. H. G., and van Wijngaarden, L., "Non-Linear Oscillations of Fluid in a Container," *Journal of Fluid Mechanics*, Vol. 22, No. 4, 1965, pp. 737–751. doi:10.1017/S0022112065001118
- [11] Chu, B.-T., and Ying, S. J., "Thermally Driven Nonlinear Oscillations in a Pipe with Travelling Shock Waves," *Physics of Fluids*, Vol. 6, No. 11, Nov. 1963, pp. 1625–1637. doi:10.1063/1.1710996
- [12] Lin, C. C., "On a Perturbation Theory Based on the Method of Characteristics," *Journal of Mathematics and Physics*, Vol. 33, 1954, pp. 117–134.
- [13] Lee, T., Zhou, Z., and Cao, Y., "Numerical Simulations of Hydraulic Jumps in Water Sloshing and Water Impacting," *Journal of Fluids Engineering*, Vol. 124, No. 1, 2002, pp. 215–226. doi:10.1115/1.1436097
- [14] Danilov, V. G., Omel'yanov, G. A., and Shelkovich, V. M., "Weak Asymptotics Method and Interaction of Nonlinear Waves, Asymptotic Methods for Wave and Quantum Problems," *Advances in Mathematical Sciences*, Ser. 2, Vol. 208, edited by M. V. Karasev, American Mathematical Society, Providence, RI, 2003, pp. 33–164.
- [15] Bauer, H. F., and Eidel, W., "Hydroelastic Vibrations in a Two-Dimensional Rectangular Container Filled with Frictionless Liquid and a Partly Elastically Covered Free Surface," *Journal of Fluids and Structures*, Vol. 19, Feb. 2004, pp. 209–220. doi:10.1016/j.jfluidstructs.2003.11.002
- [16] Kidambi, R., and Deshpande, M. D., "Liquid Sloshing in 2-Dimensional Rectangular Containers," Computational and Theoretical Fluid Dynamics Div., National Aerospace Labs., Rept. PD CF 0012, Bangalore, India, 2000.
- [17] Stoker, J. J., "Two Basic Approximate Theories," *Water Waves*, Wiley Interscience, New York, 1957, pp. 19–27.
- [18] Pyles, J. M., "An Examination of Two-Dimensional Roll Oscillations on the Liquid Dynamics of a Partially Filled Rectangular Tank," M.S. Thesis, Univ. of Cincinnati, Cincinnati, OH, Oct. 2006.
- [19] Henderson, F. M., *Open Channel Flow*, Macmillan, New York, 1966, pp. 8–75.
- [20] Defina, A., and Susin, F. M., "Stability of a Stationary Hydraulic Jump in an Upward Sloping Channel," *Physics of Fluids*, Vol. 15, No. 12, Dec. 2003, pp. 3883–3885. doi:10.1063/1.1624839